Available online at www.sciencedirect.com
SCIENCE DIRECT®
Energy Conversion and Management 47 (2006) 590–610
ENERGY CONVERSION & MANAGEMENT
www.elsevier.com/locate/enconman

Design and performance prediction of a novel zeolite–water adsorption air conditioner

D.C. Wang, Z.Z. Xia, J.Y. Wu *

Institute of Refrigeration and Cryogenics, School of Mechanical and Power Energy Engineering, Shanghai Jiao Tong University, 1954, Huashan Road, Shanghai 200030, PR China

Received 22 June 2004; received in revised form 29 October 2004; accepted 18 May 2005
Available online 18 July 2005

Abstract

A novel adsorption air conditioner is designed that supplies 8–12 °C chilled water for the fan coil in the locomotive operator cabin. Different from other two-bed adsorption cooling systems, this system has two adsorption/desorption chambers. One adsorber, one condenser and one evaporator are housed in one and the same adsorption/desorption chamber. There are no valves installed in the vacuum side. So, the reliability of the system is improved greatly. This machine uses zeolite and water as the working pairs. This system is driven by 350–450 °C exhaust gas generated by the internal combustion engine of the locomotive. The designed refrigerating power and COP (coefficient of performance) are 5 kW and 0.25, respectively, according to the requirements for the refrigeration output in the locomotive operator cabin and the waste heat provided by the engine. In this paper, a model for this system is described, and the simulation results are discussed. The model is validated in principle by limited experimental data. According to the calculation results, the refrigerating power of the machine is up to 10 kW with gas inlet temperature of 450 °C and evaporating temperature of 6.5 °C. The adsorber can be heated from 97 °C to 423 °C or cooled from 423 °C to 97 °C in 1320 s. Therefore, the heat and mass transfer performance of the adsorber is improved greatly. A few experimental data prove these conclusions.

Keywords: Adsorption; Air conditioner; Locomotive; Zeolite–water; Waste heat

* Corresponding author. Tel./fax: +86 21 62933250.
E-mail address: jywu@sjtu.edu.cn (J.Y. Wu).

0196-8904/$ - see front matter © 2005 Elsevier Ltd. All rights reserved.
doi:10.1016/j.enconman.2005.05.011

Nomenclature

C	specific heat, kJ kg^{-1} K^{-1}
COP	coefficient of performance
kF	heat transfer performance, kW K
$\dot{G}$	mass flow rate, kg s^{-1}
k_1, k_2	coefficients in adsorption equation
L	latent heat of vaporization, kJ kg^{-1}
m	mass, kg
q	isosteric heat of adsorption, kJ kg^{-1}
SCP	specific cooling power, kW kg^{-1}
T	temperature, K
x	water uptake, kg kg^{-1} adsorbent

Greek letters

τ	time, s
τ_{cyc}	cycle time, s
$\Delta\tau$	time step, s

Subscripts

a	air
ad	adsorber
c	condenser
conc	concentration
e	evaporator
eq	equilibrium
f	flow
g	gas
in	inlet
l	liquid
m	metal
out	outlet
r	refrigerant
s	saturation
v	vapour
w	water
z	zeolite
1	Chamber 1 (desorption chamber)
2	Chamber 2 (adsorption chamber)

Superscript

i	order number of interval

1. Introduction

Utilization of waste heat and solar energy is one of the main research fields for an adsorption cooling system. Solar energy is one kind of economical, clean and green energy, but it is also an unsteady energy. Its utilization is difficult and the investment of the collectors is very high. However, a large quantity of stable waste heat can be found in chemical plants, power stations and diesel engines. Such waste heat is often directly discharged into the environments today. This is not only uneconomical, but it also causes thermal pollution. Therefore, the usage of waste heat is valuable and significant. There are two kinds of available cooling machines that can utilize waste heat: absorption cooling machines and adsorption cooling machines. However, the adsorption cooling system has some advantages, such as simple structure, no rusting problem, no crystallizing problem and easily adaptable for a mobile setup. So, the adsorption cooling system is more suitable to utilize waste heat, especially the waste heat released from the diesel engine of a vehicle.

Much work [1–10] has been done in the study of adsorption air conditioning driven by waste heat. The adsorption cooling system driven by waste heat from a diesel engine has been studied by Suzuki [1] and Zhang et al. [2,3]. Suzuki's automobile adsorption air conditioner used zeolite–water as the working pairs and 400–650 °C waste heat as the driving heat source. Zhang et al. [2,3] used the waste heat generated by a 15 kW engine as the heat source and designed an adsorption cooling system with a specific cooling performance (SCP) of 32.1 W kg^{-1}. Wang [4] has compared the performance of a one-adsorber system with that of a two-adsorber system. The results show that the two-adsorber system with heat recovery has a 25% increase of the COP. Wu [5] analyzed the characteristics of the heat recovery process for a continuous adsorption heat pump with heat recovery. Saha et al. [6] designed a dual-mode silica gel–water adsorption chiller that can effectively utilize low temperature waste heat source from 40 °C to 95 °C. Their simulation results show that the optimum COP values are obtained at driving source temperatures between 50 and 55 °C in the three-stage mode and between 80 and 85 °C in the single-stage and multi-adsorber mode. Khedari et al. [7] attempted to research the feasibility of an open cycle air conditioning system using dried agricultural waste as the desiccant. Guilleminot et al. [8] used a metal matrix or a highly conductive carbon matrix to improve greatly the thermal conductivity and the permeability of the adsorbent. Miltkau and Dawoud [9] studied the influence of the thickness of the zeolite layer on the time requirements. The results showed that reducing the thickness by 1/2 results in about a 1/4 reduction of the adsorption duration and about a 1/3 reduction of the desorption duration.

All the researches mentioned above are very interesting and fundamental for utilization of an adsorption cooling system. Based on the former work, the first adsorption air conditioner for a locomotive operator cabin was built in 2002 [10–12]. This system uses zeolite–water as the working pairs and is driven by the waste heat of the exhaust gas from the internal combustion engine. It is a single-adsorber system. Jiang et al. [10] studied the dynamic characteristics and the performance of the system. As a result, the refrigerating power output is about 4 kW with the desorption temperature of 300–350 °C, the adsorption temperature of 85–10 °C, the evaporating temperature of 3–5 °C and the condensing temperature of 70–80 °C. Also, Lu et al. [11] developed an adsorption cold storage system for this air conditioner. It reduces the system starting time and keeps the

cooling output more stable, but this system has some disadvantages, such as a large volume and a lower SCP.

In this work, a novel two-adsorber continuous adsorption air conditioner is designed, which has a designed refrigerating power of 5 kW. This system has two adsorption/desorption chambers. One adsorber, one condenser and one evaporator are housed in one and the same adsorption/desorption chamber. Each adsorber has its own condenser and evaporator. There is no valve in the vacuum side, so the operating reliability of the system is greatly improved. Its performance is predicted by a uniform pressure and uniform temperature model. The results show that such system can work in a highly effective way, and the heat and mass transfer of the adsorbers satisfies the requirements.

2. System design

2.1. Design of the adsorbers

The adsorbers are the most important components for an adsorption cooling system. The performance of the adsorbers determines the capacity of an adsorption cooling system to a great extent. So, the adsorber must have good performance of the heat and mass transfer. However, the working pairs, zeolite 13X and water, have a poor thermal conductivity of 0.09–0.15 W m^{-1} K^{-1} [8,9], and therefore, enhancement of the heat transfer inside the adsorbers must be considered.

In this work, the heat transfer area is increased in order to enhance the heat transfer performance of the adsorber. At the same time, the thickness of the adsorbent layer between two fins is also decreased. Fig. 1 shows the structure of one adsorber. The copper fins with thickness of 0.12 mm are installed separately in both the adsorbent side and the air/gas side. The thickness of the adsorbent layer between two fins is about 4 mm. Therefore, the distance from the fin to the adsorbent layer center is about 2 mm, which does not exceed the 2.5 mm recommended by Miltkau and Dawoud [9]. In the adsorbent side, the mass transfer channels are designed and separated from the adsorbent layers by the wire mesh fastened to the frame. The holes with 2 mm diameter on the fins in the adsorbent side also act as the mass transfer channels, as shown in Fig. 1(b) and (c). The fins, which are aligned vertically in the adsorbent side, enhance the heat transfer between the gas/air and the metal.

Table 1 shows some parameters of the adsorbers. The adsorbent filled in the adsorbers is granular with about 1 mm in diameter. The mass flow of the air/exhaust gas is designed as 0.8 kg s^{-1}, and the velocity of air flow in the adsorber is about 4.77 m s^{-1}. The ratio between the heat capacity of the adsorbent and the heat capacity of the metal is 0.64. In each adsorber 25 kg of zeolite is filled, which is much less than that given in the literature [10–13]. Moreover, the size of the chiller is much smaller than Jiang and Lu's.

2.2. Description of the system

2.2.1. System components

The adsorber, condenser and evaporator are the main parts in the adsorption system. They are combined through welding, and no vacuum valve is installed among them, as shown in Fig. 2.

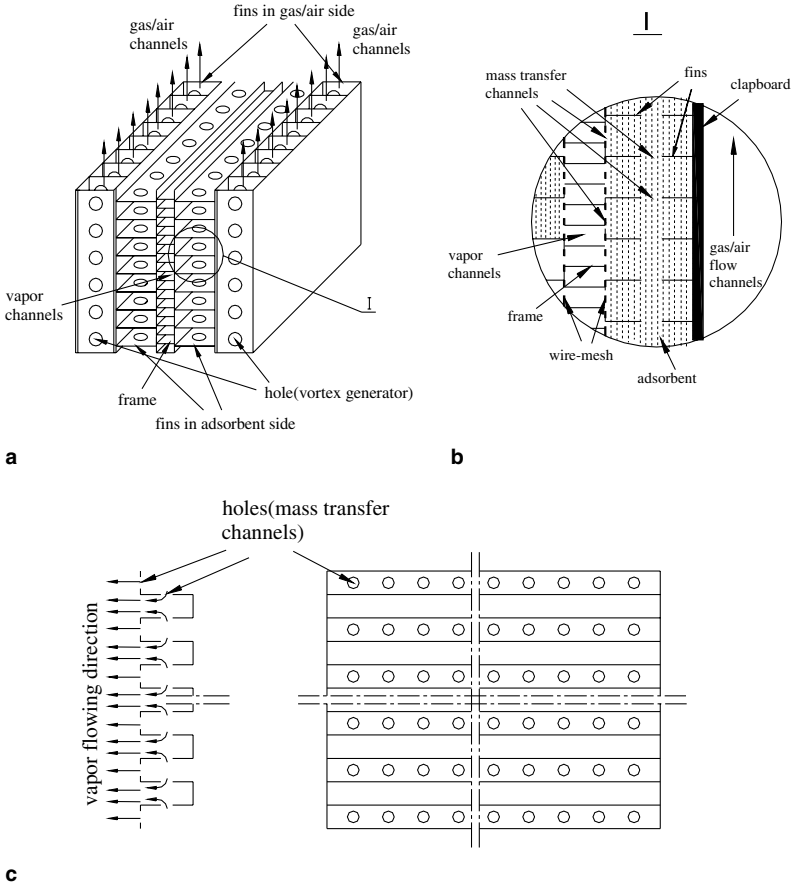

Fig. 1. The structure of the adsorber. (a) Full view, (b) partial enlarged detail and (c) fins in the adsorbent side.

Table 1
Some parameters of the adsorbers compared with Jiang and Lu's [10–13]

Name of the parameter	Value		
	In this work	In Ref.	Unit
Number of the adsorber	2	1	
Length of the adsorber	1167	1082	mm
Width of the adsorber	400	1050	mm
Height of the adsorber	200	458	mm
Metal mass of one adsorber	180	477	kg
Total heat transfer coefficient	125	10–12	$W\,m^{-2}\,K^{-1}$
Heat transfer area in adsorbent side	33.6	55	m^2/bed
Mass of adsorbent in one adsorber	25	140	kg
Total mass of refrigerant (water)	50	185	kg

This chiller combines two vacuum chambers through the air/gas switch system. Each chamber is composed of one adsorber, one condenser and one evaporator. Adsorber 1, Condenser 1 and

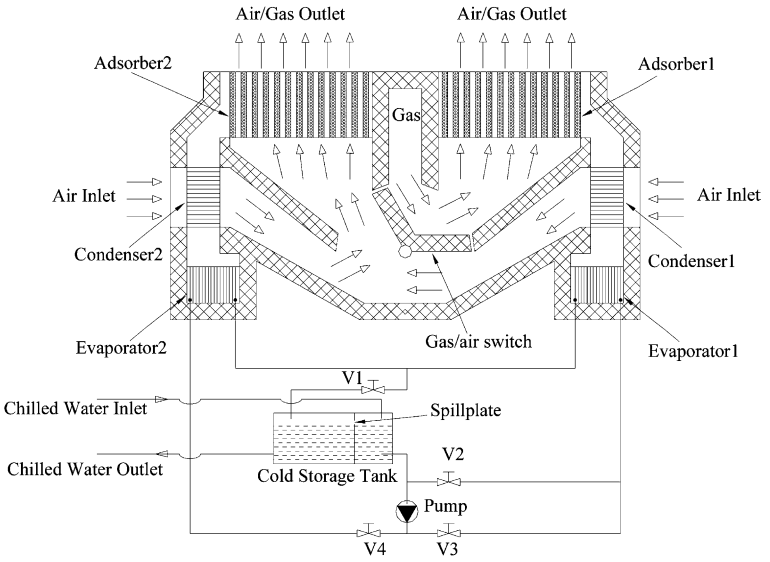

Fig. 2. Schematic diagram of the air conditioner in the locomotive operator cabin.

Evaporator 1 constitute Chamber 1. Chamber 2 consists of Adsorber 2, Condenser 2 and Evaporator 2. The switching of the adsorber between the adsorption and desorption process is performed by the gas/air switching system. Four solenoid valves are installed in the chilled water system. These valves help the evaporators switch working mode between the evaporation process and heat recovery process of the evaporators. Actually, the system is a combination of two independent single adsorber systems. The adsorber is heated by the exhaust gas from a diesel engine during the desorption process and cooled by two axial flow fans or the air flow generated by the high speed running locomotive during the adsorption process. The cooling air flow goes through

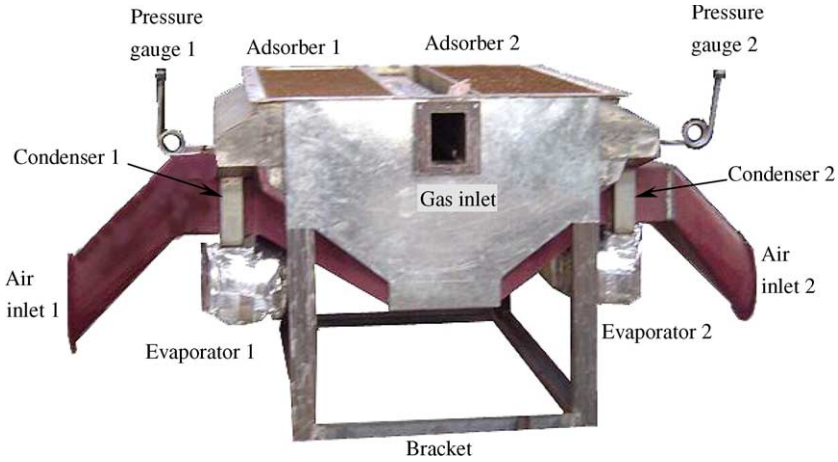

Fig. 3. Photograph of the zeolite–water adsorption air conditioner.

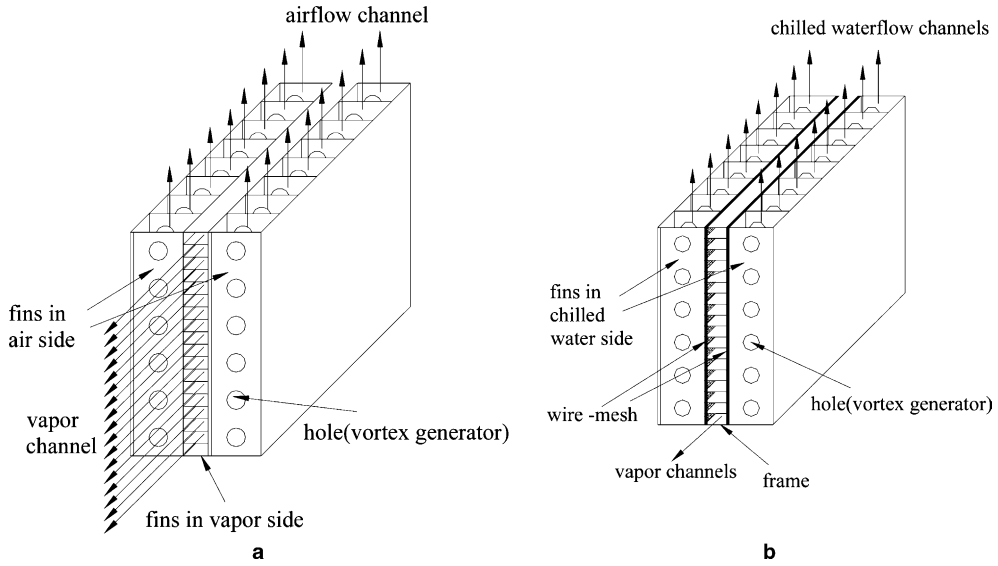

Fig. 4. Components of the adsorption air conditioning. (a) Condenser and (b) evaporator.

the condensers first and then enters the adsorber. Fig. 3 shows the picture of the prototype that has been built.

The structures of the condenser and the evaporator are shown in Fig. 4. The immersing evaporator is adopted, and its evaporating area is about 2.2 m^2. The condenser is an air-vapor heat exchanger with the condensing area of about 2.7 m^2. Both of them are plate-fin heat exchangers. The designed evaporating and condensing temperatures are 6 °C and 60 °C, respectively. A cold storage tank with 60 L water is added because the system has no refrigerating output for about 3–5 min during the switching process. The tank is divided into two parts by a spill plate. One part fills with about 40 L water as the cold storage compartment, and the other part is full of 20 L water as the backwater compartment. There are three spout holes in the spill plate that can control the water level in the horizon. The water from the evaporator goes through the cold storage compartment to the fan coil and then flows back to the backwater compartment. The backwater from the fan coil, the "warm" water (compared with the temperature of the chilled water from the evaporator), will be pumped into the evaporator and flows into the cold storage compartment after being cooled by the evaporator.

2.2.2. Principle of the system operation

The working principle of this system is much different from the system designed before [1–13]. The adsorber, condenser and evaporator are in the same vacuum chamber, as shown in Fig. 2. For each single-adsorber system, the adsorption or desorption process of the adsorber is controlled by the exhaust gas system, the air cooling system and the chilled water system in the outer circuits. The heat source from the diesel engine of a locomotive is quite sufficient. Heat recovery of the adsorbers might cause complexity of the gas/air switching system. Therefore, no heat recovery process of the adsorbers is adopted. In this work, one cycle consists of three phases:

- Firstly, the exhaust gas flows through adsorber 1, and the air flow flows through adsorber 2, as shown in Fig. 2. In this phase, adsorber 1 is heated and adsorber 2 is cooled. The desorption process will start when the pressure in one vacuum chamber becomes higher than the saturation pressure corresponding to the temperature of condenser 1 or evaporator 1. At the same time, the adsorption process will begin when the pressure in the other vacuum chamber decreases to be lower than the saturation pressure corresponding to the temperature of evaporator 2. This process continues until the desorbing or adsorbing becomes obviously weak. During this stage, valves V1 and V4 are open and V2 and V3 are closed.
- Secondly, the following phase of the cycle is the heat recovery process of the evaporators, which has a similar function to the mass recovery process generally adopted in multi-adsorber systems. In this stage, valves V1 and V3 are closed, and V2 and V4 are open. The pressure in evaporator 1 decreases quickly, and the pressure in evaporator 2 rises quickly too. The aims of this stage are to let the temperatures of evaporator 1 and evaporator 2 become identical to each other. Then, the effective adsorption/desorption time can be prolonged. A little of the refrigeration output from evaporator 2 can be saved. This phase will finish when the temperatures of the two evaporators are basically equal to each other.
- After the heat recovery process of the evaporators is over, the gas/air switching system firstly switches the exhaust gas into adsorber 2 and the air into adsorber 1. Adsorber 1 will be heated and adsorber 2 cooled. At the same time, valves V1 and V3 are opened, and valves V2 and V4 are closed. This phase is similar to the first phase except that the desorbing adsorber changes to adsorbing and the adsorbing one to desorbing. After this phase, the heat recovery process of the evaporators will repeat, like the second phase. Then, the system comes back to the original condition, and the next cycle will repeat.

The utilization ratio of the evaporator and condenser is reduced because only one condenser and one evaporator work at one time, but the reliability of system is improved greatly because there is no valve in the vacuum side.

3. Performance prediction

3.1. Mathematical model

In the simulations, a simple model based on lumped parameters is introduced. In order to simplify the analysis, some assumptions are generally made as follows:

- since the plate-fin adsorber has a high heat transfer efficiency, the temperature of the adsorbent is uniform,
- the pressure in the vacuum chamber is uniform because the mass transfer channels are more than enough in the vacuum side,
- the refrigerant is adsorbed uniformly in the adsorber and is liquid in the adsorbent,
- the heat conduction from the adsorber to the condenser and to the evaporator through the metal is neglected,
- the evaporating temperature is identical to the temperature of the liquid in the evaporator,

- leakage of the gas/air system are neglected,
- the flow rate of air is the same for the two sides, and
- the resistances to the heat and mass transfers in the adsorbent are neglected.

3.1.1. Adsorption equations

A non-equilibrium adsorption/desorption process occurs in practical adsorption cooling systems. So, a non-equilibrium adsorption equation [14] is used in the simulation.

$$\frac{dx}{d\tau} = k_1 \exp(-k_2/T_z) \cdot (x_{eq} - x) \tag{1}$$

$$x_{eq} = 0.331 \cdot \exp\left[-2.99 \cdot \left(\frac{T_z}{T_s} - 1\right)^2\right] \tag{2}$$

where k_1 and k_2 take the values of 0.019 and 906, respectively [13].

3.1.2. Governing equations

3.1.2.1. Desorption process: Chamber 1. In the beginning of the desorption process, the desorber is heated by the waste gas to begin desorbing, and the condensation process occurs firstly in the evaporator because the evaporator temperature is lower than the condenser temperature at that time. Such process will continue until the evaporator temperature rises higher than the condenser temperature. Thereafter, the condenser will be in condensing mode, and the evaporator will be idle. Therefore, in the whole desorption process, the energy equilibrium equations for each heat exchanger can be described as:

(1) Desorber:

Adsorbent: $$m_z \cdot (C_z + x \cdot C_{p,w}) \cdot \frac{dT_z}{d\tau} = (kF)_{m,z}(T_{ad,m} - T_z) + qm_z \cdot \frac{dx}{d\tau} \tag{3}$$

Metal of absorber: $$m_{ad,m}C_{ad,m} \cdot \frac{dT_{ad,m}}{d\tau} = \dot{G}_g C_{p,g}(T_{g,in} - T_{g,out}) + (kF)_{m,z}(T_z - T_{ad,m}) \tag{4}$$

Gas: $$\dot{G}_g C_{p,g}(T_{g,in} - T_{g,out}) = (kF)_{g,m} \cdot (T_g - T_{ad,m}) \tag{5}$$

(2) Condenser:

Condensate (refrigerant):

when $T_c > T_e$: (condensing process occurs in the evaporator)

$$-m_z C_{p,v}(T_z - T_c)\frac{dx}{d\tau} = (kF)_{m,v}(T_c - T_{c,m}) \tag{6}$$

when $T_c \leqslant T_e$: (Condensing process occurs in the condenser)

$$-m_z[C_{p,v}(T_z - T_c) + L(T_c)]\frac{dx}{d\tau} = (kF)_{m,wc}(T_c - T_{c,m}) \tag{7}$$

Metal of condenser: $$m_{c,m}C_{c,m} \cdot \frac{dT_{c,m}}{d\tau} = \dot{G}_{a1} C_{p,a}(T_{c,in} - T_{c,out1}) + (kF)_{m,c}(T_c - T_{c,m}) \tag{8}$$

where

$$(kF)_{m,c} = \begin{cases} (kF)_{m,v}, & T_c > T_e \\ (kF)_{m,wc}, & T_c \leqslant T_e \end{cases} \tag{9}$$

$$\text{Air}: \quad \dot{G}_{a1} C_{p,a}(T_{c,in} - T_{c,out1}) = (kF)_{a,mc} \cdot (T_{a1} - T_{c,m}) \tag{10}$$

(3) Evaporator:

Refrigerant in the evaporator:

when $T_c > T_e$,

$$[m_l + m_z \cdot (x_{conc} - x)] \cdot C_{p,w} \cdot \frac{dT_e}{d\tau} = -m_z[C_{p,v} \cdot (T_c - T_e) + L(T_e)] \cdot \frac{dx}{d\tau} - (kF)_{r,ml}(T_e - T_{e,m}) \tag{11}$$

when $T_c \leqslant T_e$,

$$[m_l + m_z \cdot (x_{conc} - x)] \cdot C_{p,w} \cdot \frac{dT_e}{d\tau} = -m_z C_{p,w} \cdot (T_c - T_e)\frac{dx}{d\tau} - (kF)_{r,ml}(T_e - T_{e,m}) \tag{12}$$

$$\text{Metal of evaporator}: \quad m_{e,m} C_{e,m} \frac{dT_{e,m}}{d\tau} = (kF)_{r,ml}(T_e - T_{e,m}) \tag{13}$$

3.1.2.2. Adsorption process: Chamber 2. In the adsorption process, the adsorber is cooled by the air flow, the condenser is idle and the evaporator is working in evaporation mode. Then, the energy equilibrium equations of the heat exchangers are expressed as follows:

(1) Adsorber:

$$\text{Adsorbent}: \quad m_z \cdot (C_z + x \cdot C_{p,w}) \cdot \frac{dT_z}{d\tau} = (kF)_{m,z}(T_{ad,m} - T_z) + q m_z \cdot \frac{dx}{d\tau} - m_z C_{p,v}(T_z - T_c)\frac{dx}{d\tau} \tag{14}$$

$$\text{Metal of adsorber}: \quad m_{ad,m} C_{ad,m} \cdot \frac{dT_{ad,m}}{d\tau} = \dot{G}_a C_{p,a}(T_{a,in} - T_{a,out}) + (kF)_{m,z}(T_z - T_{ad,m}) \tag{15}$$

$$\text{Air}: \quad \dot{G}_a C_{p,a}(T_{a,in} - T_{a,out}) = (kF)_{a,m} \cdot (T_a - T_{ad,m}) \tag{16}$$

$$\dot{G}_a = \dot{G}_{a1} + \dot{G}_{a2} \tag{16a}$$

$$T_{a,in} = (T_{c,out1} + T_{c,out2})/2 \tag{16b}$$

(2) Condenser:

$$\text{Refrigerant}: \quad m_z C_{p,v}(T_e - T_c)\frac{dx}{d\tau} = (kF)_{m,v}(T_c - T_{c,m}) \tag{17}$$

Metal of condenser: $$m_{c,m}C_{c,m}\cdot\frac{dT_{c,m}}{d\tau}=\dot{G}_{a2}C_{p,a}(T_{c,in}-T_{c,out2})+m_zC_{p,v}(T_e-T_c)\frac{dx}{d\tau} \quad (18)$$

Air: $$\dot{G}_{a2}C_{p,a}(T_{c,in}-T_{c,out2})=(kF)_{a,mc}\cdot(T_{a2}-T_{c,m}) \quad (19)$$

(3) Evaporator:

Refrigerant in the evaporator:

$$[m_e+m_z\cdot(x_{conc}-x)]\cdot c_{p,w}\cdot\frac{dT_e}{d\tau}=-m_zL(T_e)\frac{dx}{d\tau}-(kF)_{r,m2}(T_e-T_{e,m}) \quad (20)$$

Metal of condenser:

$$m_{e,m}C_{e,m}\frac{dT_{e,m}}{d\tau}=-(kF)_{r,m2}(T_{e,m}-T_e)+G_wC_{p,w}(T_{w,in}-T_{w,out}) \quad (21)$$

Chilled water: $$\dot{G}_wC_{p,w}(T_{w,in}-T_{w,out})=(kF)_{m,we}\cdot(T_w-T_{e,m}) \quad (22)$$

3.1.2.3. Heat recovery process of the evaporators. When the heat recovery process of the evaporators starts, firstly, the adsorbing adsorber is switched to desorb and the desorbing one to adsorb by the air switching system. Then, chilled water is circulated between the two evaporators. So, the models differ from the above models only in that the outlet temperature of one evaporator is the inlet temperature of the other:

$$T_{w,out1}=T_{w,in2},T_{w,out2}=T_{w,in1}$$

3.1.3. Calculation of the SCP and the COP

$$SCP=\frac{Q_{ref}}{m_z}=\frac{\int_0^{\tau_{cyc}}\dot{G}_wC_{p,w}(T_{w,in}-T_{w,out})\,d\tau}{m_z\tau_{cyc}}\approx\frac{\Delta\tau\sum\dot{G}_wC_{p,w}(T^i_{w,in}-T^i_{w,out})}{\tau_{cyc}m_z} \quad (23)$$

$$COP=\frac{Q_{ref}}{Q_h}=\frac{\int_0^{\tau_{cyc}}\dot{G}_wC_{p,w}(T_{w,in}-T_{w,out})\,d\tau}{\int_0^{\tau_{cyc}}\dot{G}_gC_{p,g}(T_{g,in}-T_{g,out})\,d\tau}\approx\frac{\sum\dot{G}_wC_{p,w}(T^i_{w,in}-T^i_{w,out})}{\sum\dot{G}_gC_{p,g}(T^i_{g,in}-T^i_{g,out})} \quad (24)$$

where τ_{cyc} is the cycle time and $\Delta\tau$ is the time step length.

4. Primary experiments for validation

Fig. 5 shows the sensors installed in the test system. The inlet and outlet temperatures of the chilled water are measured by thermal resistances #1 and #2 and the exhaust gas inlet temperature by thermal resistance #18. The air/gas temperatures in the outlet of the adsorbers are measured by thermal resistances #3, #4, #5 and #6. The thermal resistances in the condensers or the

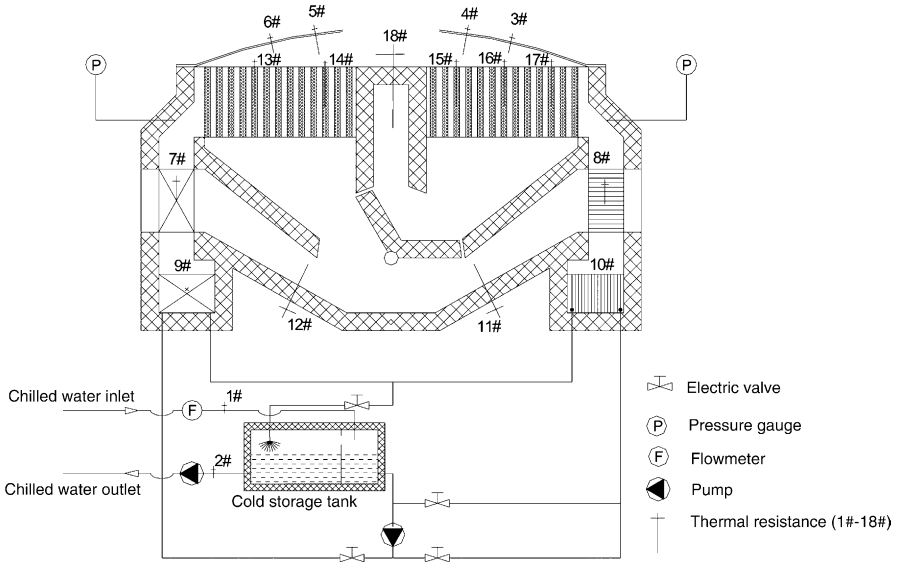

Fig. 5. Sensors layout in the zeolite–water air conditioner.

evaporators are tightly bound to the condensation surface or to the evaporation surface. All the thermal resistances in the system are 4-wire Pt100 type, of which the deviations are $0.3 + 0.005t$ °C (t is the tested temperature value). The flow rates of the air and exhaust gas are measured by a pitot tube flow meter with an accuracy of 1.5%. The flow rate of the chilled water is measured by a revolving flow meter with an accuracy of 0.1%.

All the data are acquired by a Keithly 2700 Multimeter/Data Acquisition System interfaced with a PC. The SCP and COP are calculated by Eqs. (23) and (24), respectively. Then, deviations of SCP and COP generated by the error of the measurements are, respectively, 0.6% and 2.1%.

5. Results and discussions

5.1. Comparisons with experimental results

In this work, only a few experimental data are obtained for the experimental work failed due to the high leakage of one condenser. However, the temperatures of the adsorber, the condenser and the evaporator are measured. The refrigerating power and COP of one adsorption/desorption chamber are, respectively, 3.2 kW and 0.152 with the evaporating temperature of 8 °C based on the experimental results.

Fig. 6 shows the curves of the evaporator temperature variations with operating time, and Fig. 7 shows the condenser temperature variations with operating time. The heat transfer performance of the adsorber has also been tested, as shown in Fig. 8(a). All the data shown in these figures are obtained from the experiments and the simulations for a cycle without a heat recovery process of the evaporators. In terms of these figures, the simulation results are basically consistent with the experimental results. In view of the influence of the assumptions in the model on the

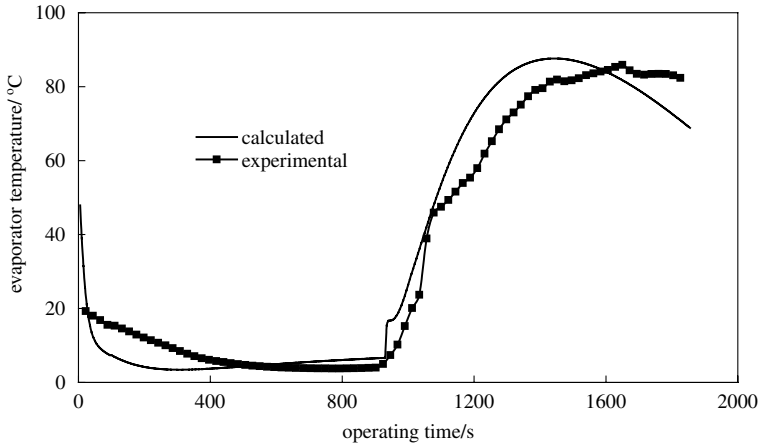

Fig. 6. Evaporator temperature variations with operating time.

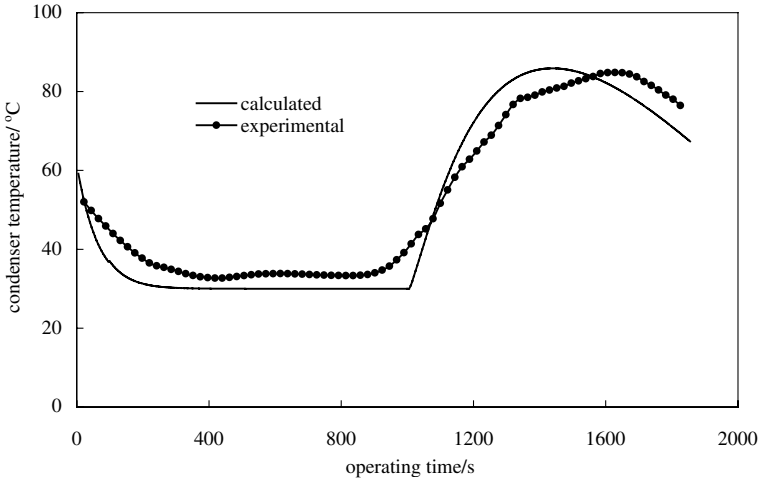

Fig. 7. Condenser temperature variations with operating time.

simulation results, it can be concluded that the model used in this work is validated to a certain extent though the experimental results offered in the paper are not quite enough to validate all aspects of the model.

Fig. 8(b) is obtained from the literature [13]. Comparisons between Fig. 8(a) and (b) testify that such structure of the adsorber greatly improves the heat transfer performance of the adsorber.

5.2. Calculated results analysis

Figs. 9 and 10 show the calculated temperature variations of the adsorbent and the evaporator metal in one cycle, respectively. These figures are all based on the same case. In this case, the heat

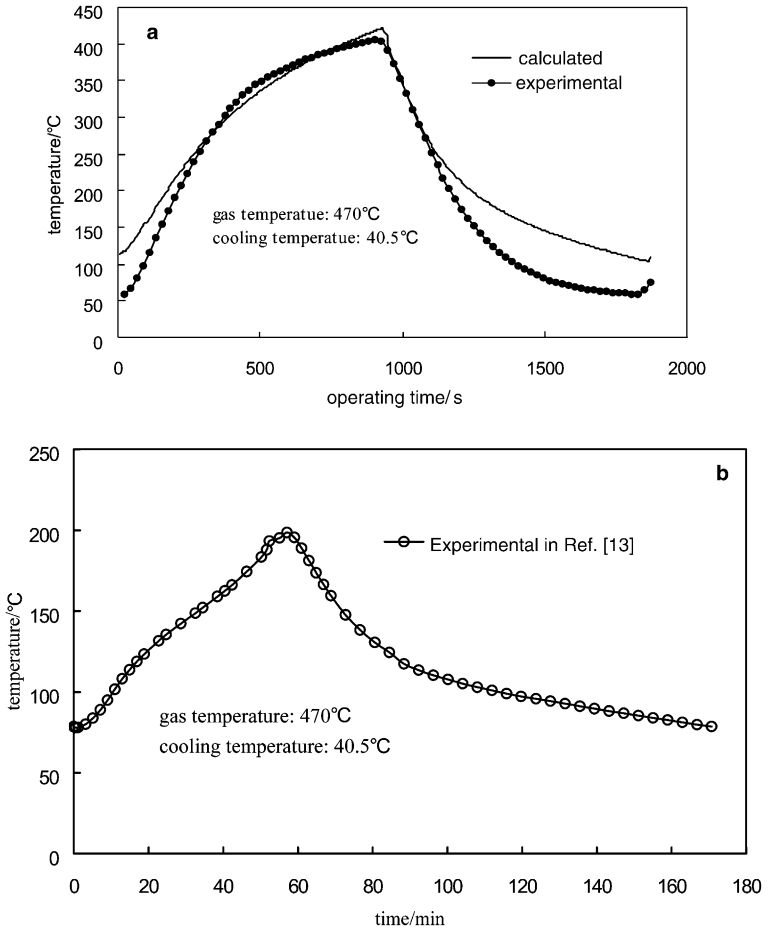

Fig. 8. Adsorber temperature variations with operating time (cycle time: 1770 s, no evaporator heat recovery). (a) In this work and (b) in Ref. [13].

source temperature is 450 °C, the cooling air temperature is 40 °C, the chilled water temperature is 10 °C and 2640 s cycle time with 40 s heat recovery time of the evaporator are adopted.

The temperature of the adsorbent changes from 97 °C to 423 °C in 1320 s. The rate of temperature rise is about 14.8 °C min^{-1}. The heating time is shortened by 1680 s and the cooling time is shortened by 6000 s compared with the case when the temperature changes between 80 °C and 201 °C in the literature [13], as shown in Fig. 8(b). The heat transfer performance is greatly improved. The temperature of the adsorbent in the desorber drops sharply at first and then rises gradually during the heat recovery process of the evaporators, as shown in Fig. 9. On the contrary, the temperature in the adsorber rises sharply at first and then drops gradually. These phenomena can be explained as follows. For the desorber, firstly, the temperature of the evaporator sharply declines during the heat recovery process of the evaporators, as shown in Fig. 10. Then, the pressure in the desorber decreases promptly. Much water will be quickly desorbed from the adsorbent, and much desorption heat will be needed. However, time is necessary to transfer heat

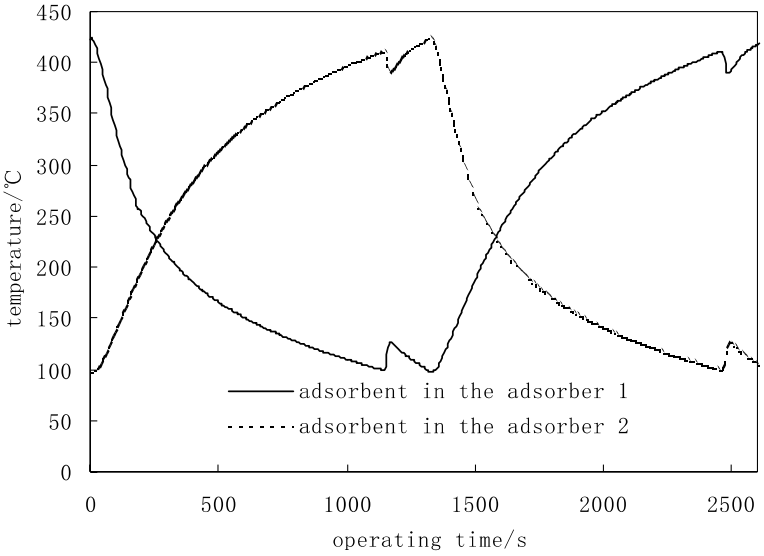

Fig. 9. Temperature variation of the adsorbent in one cycle.

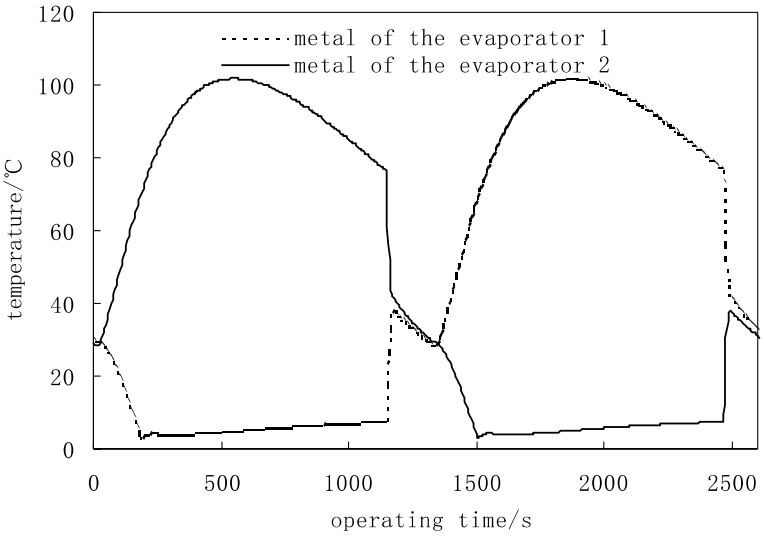

Fig. 10. Temperature variation of the evaporator metal in one cycle.

from the exhaust gas to the adsorbent. Therefore, the desorption heat cannot be offset in time so that the temperature of the adsorbent in the desorber decreases quickly. The temperature of the adsorbent rises again when the heat transferred from the exhaust gas becomes more than the desorption heat. For the adsorber, the heat recovery of the evaporators causes a sharp increase of the pressure in the evaporator of the adsorbing side, and much water is adsorbed by the adsorbent. Then, much adsorption heat is released to cause a sharp increase of the temperature of the

adsorbent. This temperature will decrease again when the heat taken away by the cooling air becomes more than the adsorption heat. These phenomena indicate that the adsorber is very sensitive to the pressure in the evaporator. Namely, the adsorber has a nicer mass transfer performance.

It is unavoidable that the temperature of the condensate is very high in an air cooling zeolite–water system. The temperature of the evaporator metal is up to 101.8 °C as well as the condensate temperature during the desorption process, but the minimum temperature is only 2.8 °C (0.9 °C lower than the metal temperature) during the adsorption process. So, a high temperature of the condensate causes more refrigerating power loss. This impact cannot be avoided for a system whose condenser, evaporator and adsorber are enclosed in one chamber. The pressure inside them is almost identical at all times. It is difficult to ensure a lower condensing temperature because the condensation process happens not only in the condenser but also in the evaporator. Therefore, it is necessary to take account of the heat recovery process of the evaporators. There are two reasons: one is that the heat recovery process of the evaporators can effectively decrease the temperature of the evaporator in the desorbing side and reduce the loss of refrigerating power. The other is that the heat recovery process of the evaporators can increase the temperature of the evaporating evaporator and make the adsorber adsorb more refrigerant. The decrease of the metal temperature (as shown in Fig 10) indicates that the evaporating ability is still powerful during the heat recovery process of the evaporators. There are about 3 min in which no refrigeration is produced. So, the cooling storage ability of the chilled water system is necessary.

Fig. 11 shows the performance of the system when the heating/cooling time changes from 360 s to 1740 s. In these cases, the heat recovery time of the evaporator is 180 s and the cycle time is equal to two times the heat recovery time of the evaporator plus the heating/cooling time. In the figure, the COP rises with the increase of cycle time because the longer cycle time causes lower heating power, but the refrigerating power rises first and decreases last. The highest refrigerating power is about 9.52 kW when the cycle time is about 2480 s. So, the optimal cycle time for the system is 2480 s if the refrigerating power is more important and the heat source is enough,

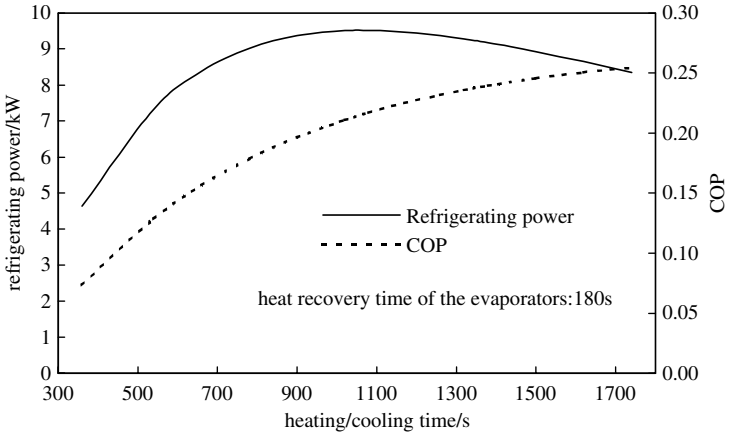

Fig. 11. COP and the refrigerating power with the heating/cooling time (water temperature: 10 °C; cooling air temperature: 40 °C; gas temperature: 450 °C).

though the COP is only 0.217 at that time. Longer cycle time (longer than 2480 s) will be necessary if the heat source is insufficient and a high COP is needed.

According to Jiang and Lu [10–13], the adsorption time is more than 7200 s and the desorption time is more than 3000 s, as shown in Fig. 8(b). So, the designed adsorption system in this work is much better and has a quite fine performance of heat and mass transfer. There is only a little lower COP, by about 0.03, than Jiang and Lu's for the switch frequency of the system in this work is higher.

Table 2 shows the COP of the system with different heating/cooling time and different heat recovery time of the evaporator. Table 3 shows the corresponding refrigerating power. The main objective of evaporator heat recovery is to decrease the pressure in the desorbing adsorber more quickly to save some refrigerating power of the evaporator that is just finishing the evaporation process. Then, the effective adsorption time will be prolonged, but too long heat recovery time of the evaporator will counteract the effect of the evaporator heat recovery and even cause an opposite effect. The temperatures of the two evaporators are not close to each other, and the potential of the evaporator heat recovery is not exerted fully if the evaporator heat recovery time is too short. However, the effective adsorption time will be shortened if the evaporator heat recovery

Table 2
COP of the system (chilled water temperature: 10 °C; cooling air temperature: 40 °C; gas temperature: 450 °C)

Heat recovery time of evaporator (s)	Heating/cooling time (s)					
	760	880	1000	1060	1120	1180
0	0.15621	0.17673	0.19368	0.20099	0.20759	0.21358
30	0.18288	0.20214	0.21729	0.22354	0.22902	0.23382
60	0.18468	0.20328	0.21778	0.22374	0.22896	0.23354
90	0.18453	0.20276	0.21697	0.22283	0.22799	0.23255
120	0.18306	0.20106	0.21521	0.22110	0.22632	0.23096
150	0.18099	0.19883	0.21308	0.21905	0.22439	0.22916
180	0.17867	0.19643	0.21084	0.21694	0.22241	0.22734
210	0.17630	0.19404	0.20863	0.21487	0.22050	0.22558

Table 3
Refrigerating power of the system (water temperature: 10 °C; cooling air temperature: 40 °C; gas temperature: 450 °C)

Evaporator heat recovery time (s)	Heating/cooling time (s)					
	760	880	1000	1060	1120	1180
0	8.4620	9.0009	9.3078	9.3919	9.4374	9.4494
30	9.5762	10.0033	10.1919	10.2151	10.1990	10.1496
60	9.5558	9.9522	10.1117	10.1221	10.0951	10.0367
90	9.4720	9.8498	9.9943	9.9989	9.9680	9.9072
120	9.3404	9.7062	9.8450	9.8488	9.8178	9.7585
150	9.1868	9.5433	9.6817	9.6868	9.6585	9.6023
180	9.0226	9.3719	9.5129	9.5210	9.4961	9.4445
210	8.8544	9.1988	9.3432	9.3546	9.3341	9.2873

time is too long. About 40 s of evaporator heat recovery time is the best for the COP and the refrigerating power of the system.

The variations of the COP and the refrigerating power with the chilled water temperature and the cooling air temperature are all linear, as shown in Figs. 12 and 13. A higher chilled water temperature results in a higher COP and a higher refrigerating power, but a higher cooling air temperature results in a lower COP and a lower refrigerating power. The COP and the refrigerating power are 0.2237 and 10.184 kW, respectively, for the designed working condition whose the gas temperature is 450 °C, the cooling air temperature is 40 °C and the chilled water temperature is

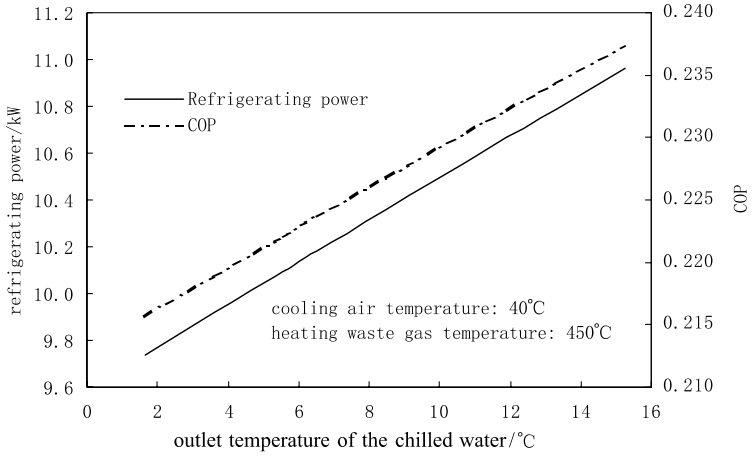

Fig. 12. COP and refrigerating power with outlet water temperature (cycle time: 2480 s; evaporator heat recovery time: 40 s).

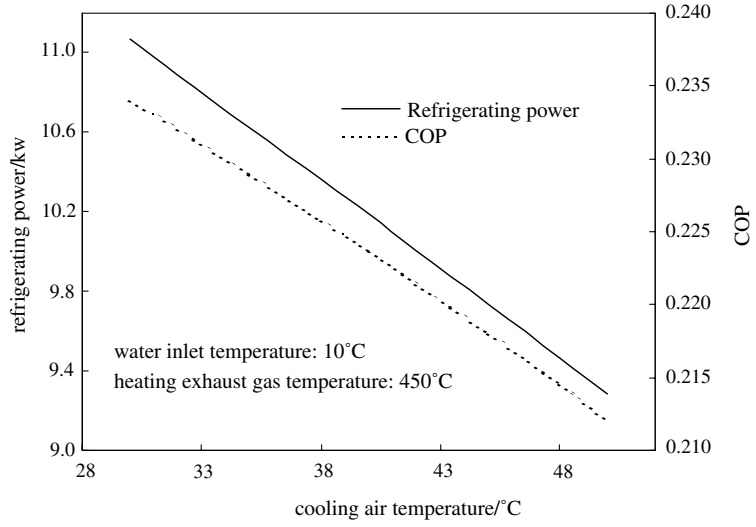

Fig. 13. COP and refrigerating power with cooling air temperature (cycle time: 2480 s; evaporator heat recovery time: 40 s).

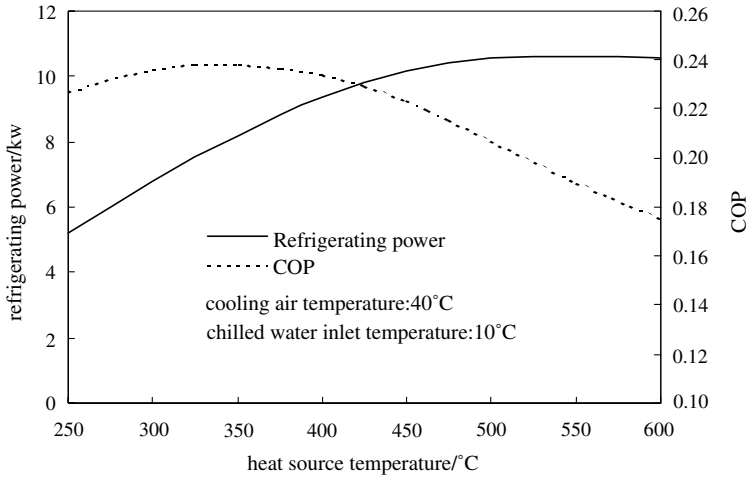

Fig. 14. COP and refrigerating power with heat source (exhaust gas) temperature (cycle time: 2480 s; evaporator heat recovery time: 40 s).

6.5 °C. The heat recovery time of 40 s and heating/cooling time of 1060 s are adopted under the designed working condition.

The heat source temperature has different influences on the COP and the refrigerating power, as shown in Fig. 14. A higher heat source temperature is advantageous for a better desorption process. More water will be desorbed from the adsorber, and the cycle adsorption mass is increased. Then, the refrigerating power will increase with the rise of the heat source temperature, but the refrigerating power will change little if the heat source temperature is higher than 500 °C because the zeolite will almost contain no water at a temperature higher than 350 °C, and the excessively high temperature of the adsorber will become a heavy burden for the cooling and heating. The adsorbent will be effectively destroyed and lose its adsorption ability. The adsorbent temperature can be controlled at a lower value by means of control of the heating time, but it will render the cooling time insufficient or cause the adsorbers to work discontinuously. So, a higher than 500 °C heat source is unnecessary and uneconomical. As for the COP, it will decrease if the heat source temperature is higher than 340 °C because a temperature higher than 340 °C causes more increase of the heating power than that of the refrigerating power. Therefore, the recommended heat source temperature is between 340 °C and 500 °C for this system when the heating time is 1060 s.

6. Conclusions

The designed adsorption cooling system in this work has a rather fine performance of heat and mass transfer. So, little adsorbent is needed and a shorter cycle time can be adopted. According to the prediction, more than 10 kW refrigerating power is achieved when the heating/cooling time is 1060 s and the heat recovery time of the evaporator is 40 s under the standard working condition whose heat source temperature is 450 °C, cooling temperature is 40 °C and chilled water temperature is 10 °C.

The heat and mass transfer of the adsorber is vital to improving the performance of an adsorption cooling system. High performance of the heat and mass transfer leads directly to less adsorbent filled in the adsorber, a lighter weight of the adsorber and a shorter cycle time. Then, the SCP of the system increases greatly though the COP decreases a bit. The SCP reaches 200 W kg^{-1} adsorbent (in two adsorbers) and is 164 W kg^{-1} adsorbent higher than that of Jiang and Lu's [10–13]. The calculation results also indicate that such a system structure as in this work is more effective than that designed before. So, this system has rather high potential.

7. Challenge

The adsorption air conditioning designed in this work still has some key problems. It requires a high welding technique to keep a high vacuum level in the chambers. The leakage from the exhaust gas flow side to the air flow side in the air/gas switch system is difficult to be avoided. The heat transfer from the heated adsorber to the condenser and even to the evaporator through the heat conduction of the metallic shell cannot be avoided. The adsorber, the condenser and the evaporator are in one vacuum chamber and are not separated in the vapor channel from each other, and so, condensing may occur in the evaporator. Therefore, more refrigeration power loss is generated. Further improvements are undergoing at present.

Acknowledgments

This work is supported by the National Science Fund for Distinguished Young Scholars of China under Contract No. 50225621 and the state Key Fundamental Research Program under Contract No. G2000026309.

References

[1] Suzuki M. Application of adsorption cooling systems to automobiles. Heat Recovery Syst CHP 1993;4(13):335–40.
[2] Zhang LZ, Wang L. Performance estimation of an adsorption cooling system for automobile waste heat recovery. Appl Thermal Eng 1997;12(17):1127–39.
[3] Zhang LZ. Design and testing of an automobile waste heat adsorption cooling system. Appl Thermal Eng 2000;1(20):103–14.
[4] Wang RZ. Performance improvement of adsorption cooling by heat and mass recovery operation. Int J Refrigeration 2001;7(24):602–11.
[5] Wu JY, Wang RZ, Xu YX. Dynamic analysis of heat recovery process for a continuous heat recovery adsorption heat pump. Energy Convers Manage 2002;16(43):2201–11.
[6] Saha BB, Koyama S, Kashiwaqi T, Akisawa A, et al. Waste heat driven dual-mode, multi-stage, multi-bed regenerative adsorption system. Int J Refrigeration 2003;7(26):749–57.
[7] Khedari J, Rawanqul R, Chimchavee W, et al. Feasibility study of using agriculture waste as desiccant for air conditioning system. Renew Energy 2003;10(28):1617–28.
[8] Guilleminot JJ, Chalfen JB, Choister A. Heat and mass transfer characteristics of composite for adsorption heat pumps. Int Absorp Heat Pump Conf, AES 1993;31:401–6.
[9] Miltkau T, Dawoud B. Dynamic modeling of the combined heat and mass transfer during the adsorption/desorption of water vapor into/from a zeolite layer of an adsorption heat pump. Int J Thermal Sci 2002;41:753–62.

[10] Jiangzhou S, Wang RZ, Lu YZ, Xu YX, Wu JY. Experimental investigations on adsorption air-conditioner used in internal-combustion locomotive driver-cabin. Appl Thermal Eng 2002;22:1153–62.
[11] Lu YZ, Jiangzhou S, Wang RZ, Xu YX, Wu JY. Adsorption cold storage system with zeolite–water working pair used for locomotive air-conditioning. In: Proceedings of international sorption heat pump conference, Shanghai, China, 24–27 September 2002. p. 484–9.
[12] Jiangzhou S, Wang RZ, Lu YZ, Xu YX, Wu JY, Li ZH. Locomotive driver cabin adsorption air-conditioner. Renew Energy 2003;11(28):1659–70.
[13] Lu YZ. Adsorption air-conditioning system with zeolite–water working pair powered by waste heat of fuel gas exhausted from Diesel locomotive. PhD dissertation. Submitted to Shanghai Jiaotong University, 2002.
[14] Sakada A, Suzuki M. Fundamental study on solar powered adsorption cooling system. J Chem Eng Jpn 1984;17:52–7.